Bull. Inst. Chem. Res., Kyoto Univ., Vol. 57, No. 2, 1979

Structural Changes of Polyethylene Single Crystal due to Electron Irradiation

Akiyoshi KAWAGUCHI*

Received April 3, 1979

The thickness of polyethylene single crystal mat decreases with the increase of electron irradiation while its width increases. The resultant macroscopic volume of mat decreases at the initial stage of irradiation and decreases with further irradiation. Being in line with the volume change, the observed macroscopic density increases at low radiation doses and decreases at high radiation doses. However, the crystalline density obtained from the X-ray measurement shows the monotonical decrease with irradiation. The wide angle X-ray diffraction pattern becomes blurry and broad with the increase of radiation dose and simultaneously the discrete small angle X-ray diffraction is less intense and disappears when the crystallinity of mat is lost. The annealing behavior of irradiated mats differs from one another depending on how they are damaged by radiation. The lattice spacing d_{200} and the half-value breadth, which increase with irradiation, increase further by annealing at rather low temperature and decrease at the temperature above a certain temperature. These observations of changes in crystalline state by electron irradiation and subsequent annealing are interpreted in terms of the change in molecular orientation in a lamella, the decrease of interlamellar distance and the introduction of various defects in crystalline core which are caused by *interlamellar* and *intralamellar* cross-linking.

KEY WORDS: Cross-linking / Density / X-ray diffraction / Lattice spacing / Half-value breadth /

INTRODUCTION

Radiations serve as a source for improving the nature of substances to some extent and also have a harmful influence on them. Thus the effects of various radiations on organic substances including polymers have been extensively examined in the field of radiation chemistry.[1] Cross-linking produced between polymer chains by irradiation prevents the plastic flow of the melt and then polymers thus cross-linked have been utilized for the study of structures and properties associated with melts, for example the crystallization of polymers induced under the strain,[2] annealing of polymer crystals.[3] Polymer crystals are not inherently perfect but distorted, *i.e.* crystals are in paracrystalline state. For example, ionizing radiation produces more lattice distortion in polymer crystals so as to reveal the nature of lattice distortion as well as the properties of cross-links.[4,5] Since polymer crystals are very sensitive to electron radiation, the degradation of polymers or the collapse of crystal structure by electron beam limits the application of electron microscopy to polymer system. It is clear from a variety of examinations by many workers[6-9] that the electron radiation damage of polymer crystals can be reduced by the use of cooling of specimen, low electron radiation dose rate and higher accelerating voltage.

* 河口昭義: Laboratory of Polymer Crystals, Institute for Chemical Research, Kyoto University, Uji, Kyoto-Fu, 611.

The image intensifier is introduced to reduce the electron damage which causes a structural change of polymer crystals.[10] In the present paper, the structural change of polyethylene single crystal due to electron irradiation is examined, although the main attention is drawn to the change in the superstructure or lamellar structure.

EXPERIMENTAL

Polyethylene used in the present work was an un-fractionated high-density polyethylene Sholex 6050. Single crystals were isothermally grown from the 0.05 wt% solution in *p*-xylene. Thin mats of thus prepared single crystals were formed by sedimentation and slow filteration. Mats were fully dried in the ambient atmosphere at room temperature and kept in a vacuum at 80°C for 24hrs. to remove the residual solvent.

Electron irradiation was carried out using a high voltage (300 kv) electron microscope according to the same procedure as Nagasawa and Kobayashi had employed.[4] Single crystal mats were covered with thin polyethylene films so that they were placed at the position where radiation damage was maximum, *i.e.* at the depth of 0.25 mm at 200 kv. A large amount of irradiated specimen was needed to make various examinations and the irradiation experiment was carried out twice. The irradiation conditions are shown in Table I for these two series of experiments; A and B. As various radicals are formed by electron irradiation, specimens were kept in a vacuum for more than 24 hrs. after completion of irradiation so that radicals were died out by the formation of cross-link, double bond *etc.* among molecular chains. However, oxydization of specimen could not completely avoided as carboxylic, carbonyl, hydroxyl *etc.* groups were found to exist in irradiated specimens from the infrared spectroscopic measurement. For the comparison with single crystal mats, drawn films were also irradiated in a similar way.

Table I. Conditions for Electron Irradiation.

Accelerating voltage 200 KV						
A: Current density 0.29 μA/cm^2						
Specimen	No. A1	No. A2	No. A3	No. A4	No. A5	No. A6
Radiation time (min.)	0	60	120	240	480	960
Radiation dose $\times 10^4$(coulomb/cm)	0	10.5	21.0	42.0	84.0	168
B: Current density 0.28 μA/cm^2						
Specimen	No. B1	No. B2	No. B3	No. B4	No. B5	No. B6
Radiation time (min.)	0	30	60	120	240	480
Radiation dose $\times 10^4$(coulomb/cm^2)	0	6.3	12.6	25.2	50.4	100.8

Annealing of un-irradiated and irradiated specimens were carefully carried out in nitrogen atmosphere to prevent them from oxidizing.

Specimens thus prepared were examined by the wide and small angle X-ray diffraction, infrared spectroscopy, differential scanning calorimetry(DSC) and density measurement. The X-ray diffraction experiment was carried out with Ni–

filtered Cu-Kα ray.

RESULTS AND DISCUSSION

Density and crystallinity

A series of photographs in Fig. 1 shows the change of the shape of single crystal mat with irradiation. It is clearly seen that a thin mat crumpled and crushed with irradiation for a prolonged period. This phenomenon results from the increase of the width of specimen and the decrease of thickness. The change in width and thickness are listed in Table II. R values in Table II are calculated by following equation:

$$R = (1+\text{rate of increase in width})^2 \times (1-\text{rate of decrease of thickness}) \quad (1)$$

which defines the ratio of the overall volume of irradiated mat to that of un-irradiated one. The R value slightly decreases with radiation of the dose up to 0.00252 coulomb/cm^2 and increases with further irradiation. As for drawn polyethylene, the specimen was broken down even at moderate irradiation because of large shrinkage so that the change in volume could not be examined. Grubb, Keller, and Groves have observed the increase of the area of lamellar single crystal by electron irradiation with electron microscope and found that the linear expansion amounted to 22 %-24 %, when the single crystal was at the final state of irradiation damage by electron beam[11]. The linear expansion or the increase of width of lamellar crystal just before the crystallinity is lost is estimated at about 10 % from their electron microscopical data

Table II. The Thickness, Width and R Value of Various Polyethylene Single Crystal Mats of Series B

Specimen	No. B1	No. B2	No. B3	No. B4	No. B5	No. B6
Decrease in thickness (%)	0	0	1.7	10.2	12.7	12.0
Increase in width (%)	0	0	1.0	2.0	9.3	19.6
R value	1.0	1.0	0.97	0.95	1.03	1.2

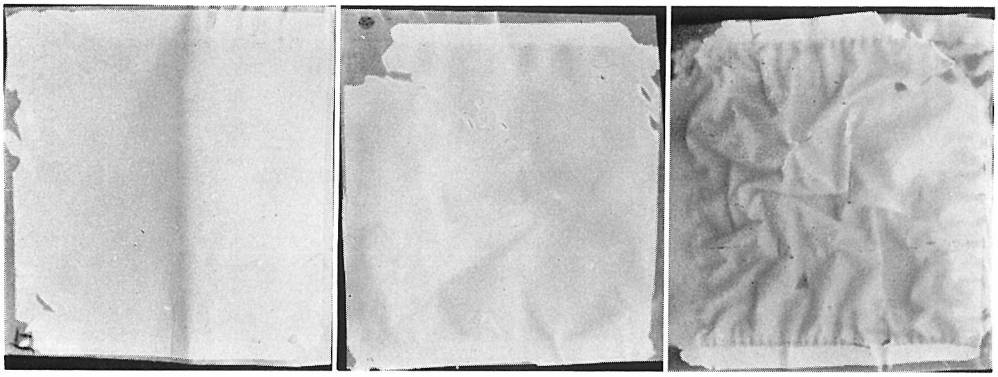

(a) (b) (c)

Fig. 1. Optical photographs of various polyethylene single crystal mats; (a) No. A1, (b) No. A4 and (c) No. A6.

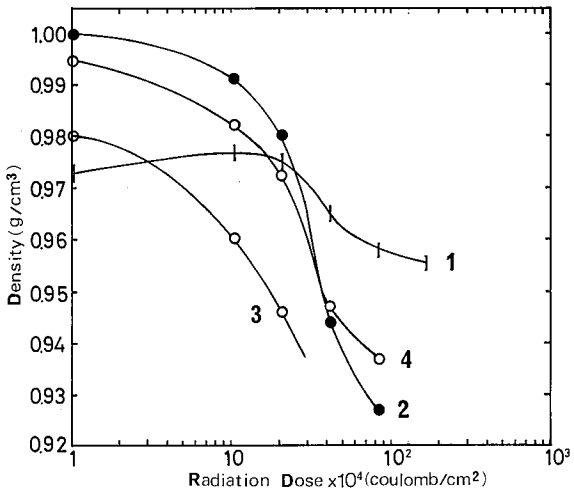

Fig. 2. Density as a function of radiation dose; (1) the observed density of polyethylene single crystal mat, (2) the crystalline density calculated on the basis of X-ray diffraction data, and the densities of mat calculated by eq.(2) for $\rho_a=0.86$ (3) and for $\rho_a=0.955$ (4)

and the value is in good agreement with the present macroscopical value.

The change in density due to irradiation is shown in Fig. 2. The density was measured using a density gradient tube consisting of the mixture of water and ethylalcohol. The density slightly increases with radiation of the dose up to 0.002 coulomb/cm^2, and then decreases as the radiation dose increases further. Eventually the density levels off. The reciprocal of R value is proportional to the density and the density calculated from the R value on the basis of the density of un-irradiated mat has a similar dose dependence as the observed density.

Table III shows lattice spacings d_{200}, d_{020}, and d_{002} and the degree of crystallinity of the sample of series A. The degree of crystallinity was measured according to the method adopted for an oriented specimen by Nukushina.[12] The crystal density can be calculated using these lattice spacings and is plotted in Fig. 2. If the decrease of the degree of crystallinity is due simply to the conversion of crystal to the amorphous state, the density can be estimated using data in Table II by the equation

$$\rho_{cal} = \rho_c w_c + \rho_a (1 - w_c) \qquad (2)$$

where ρ_c, ρ_a, and w_c denotes the densities of crystalline and amorphous states and the degree of crystallinity, respectively. The densities thus calculated are shown in Fig. 2 (curve 3 for $\rho_a=0.86$ which is estimated from the density of polyethylene melt; curve 4 for $\rho_a=0.955$ which is the observed value of the mat converted into an amorphous state by irradiation). The discrepancy between the observed and calculated densities proves that the assumption is not always valid. In spite of the decrease of the degree of crystallinity and crystal density, the observed density increases as for specimens irradiated at rather low radiation doses. This increase of density is considered to be due to the decrease of the content of void in specimen. This speculation is quite likely as seen from the change in R value.

X-ray measurement

Figure 3 shows the change of wide and small angle X-ray diffraction photographs of single crystal mats with electron irradiation. The wide angle X-ray diffraction pattern(WAXD) is broad and blurry with the increase of radiation dose and eventually becomes a halo indicating the amorphous structure. Concurrently, the discrete small angle X-ray diffraction (DSAXD) is less intense with the increase of radiation dose and dies out when the WAXD changes into a halo ring. However, only the oval-shaped diffuse scattering in small angle X-ray diffraction which trails from the center in the meridial direction is vaguely observed, even after the crystallinity is lost at longer irradiation. These changes in both WAXD and DSAXD show that the crystalline texture, *i.e.* superstructure, also collapses by electron irradiation, when crystals are converted into an amorphous state.

As previously reported by Nagasawa and Kobayashi, lattice spacings d_{200} and d_{020} expand at high radiation doses (see Table III). The d_{002} spacing tends to

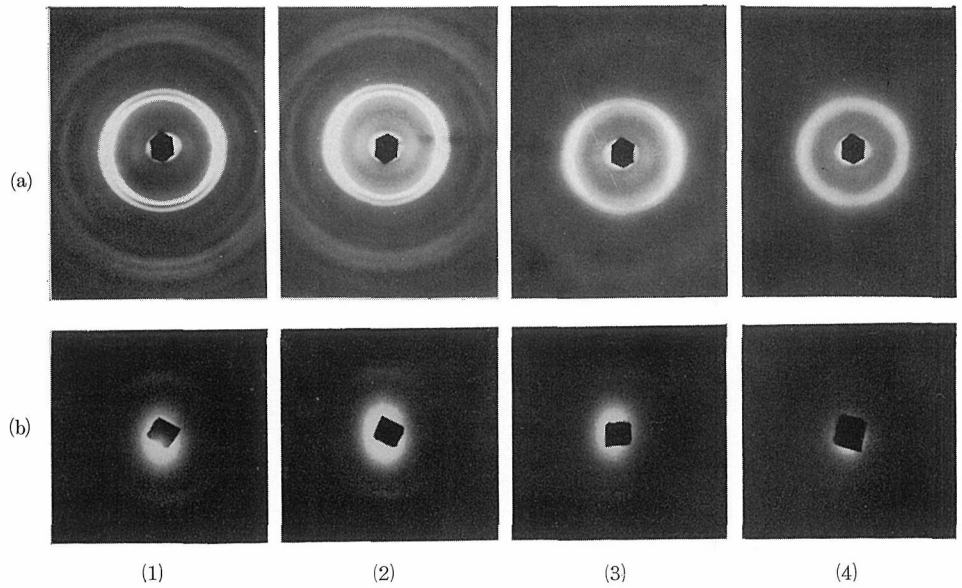

Fig. 3. (a) Wide and (a) small angle X-ray diffraction photographs taken of various polyethylene single crystal mats; (1) No. A1, (2) No. A3, (3) No. A5 and (4) No. A6. Mats are set in such a way that the normal of mat is vertical in these photographs and that the incident direction of X-ray is parallel to mat surface.

Table III. Lattice Spacings, d_{200}, d_{020} and d_{002}, and the Degree of Crystallinity of Various Polyethylene Single Crystal Mats of Series A

Specimen	No. A1	No. A2	No. A3	No. A4	No. A5	No. A6
Lattice spacing (Å)						
d_{200}	3.72	3.73	3.74	3.85	3.91	amorphous
d_{020}	2.46	2.48	2.49	2.51	2.53	
d_{002}	1.271	1.275	1.273	1.274	1.268	
Degree of crystallinity (%)	88.5	75.2	66.3	66.0	46.0	

expand slightly at low radiation doses (specimen of Nos. A2, A3, and A4) and contract for the specimen rather highly irradiated (specimen of No.A5). It is difficult to measure the molecular orientation in single crystal mats so that the birefringence of drawn films have been measured to see the change in molecular orientation due to electron irradiation. The birefringence increases with irradiation dose for the specimens of Nos. A3 and A4, *i.e.* the molecular orientation in them increases, and decreases with further irradiation (see Table IV). The drawn film which has large birefringence shows the expansion of d_{002} spacing and the specimen with low birefringence due to further irradiation shows a small d_{002} spacing. This may be interpreted in terms of the change of the strain imposed on stem segments in the crystal. When cross-links are produced between stem segments in the crystal by irradiation (*intralamellar cross-linking*) as Nagasawa and Kobayashi proposed, then a force is exerted on the stem segment to pull it in along its direction. Since the stem segment is anchored at the fold surface, the strain may be imposed on it and produce the expansion of d_{002} spacing as well as the increase of molecular orientation.

Figure 4(a) shows the relative intensity curves of DSAXD normalized as follows: the diffraction curves measured in the vertical direction in Fig. 3(b) were standard-

Table IV. *Birefringence of Drawn Polyethylene Depending on Radiation Doses*

Radiation dose $\times 10^4$ (coulomb/cm^2)	0.0	10.5	21.0	42.0	84.0	168.0
Birefringence $\times 10^2$	1.6	1.5	1.8	1.9	1.1	1.1*

* The specimen was broken down and did not show the crystalline X-ray diffraction pattern.

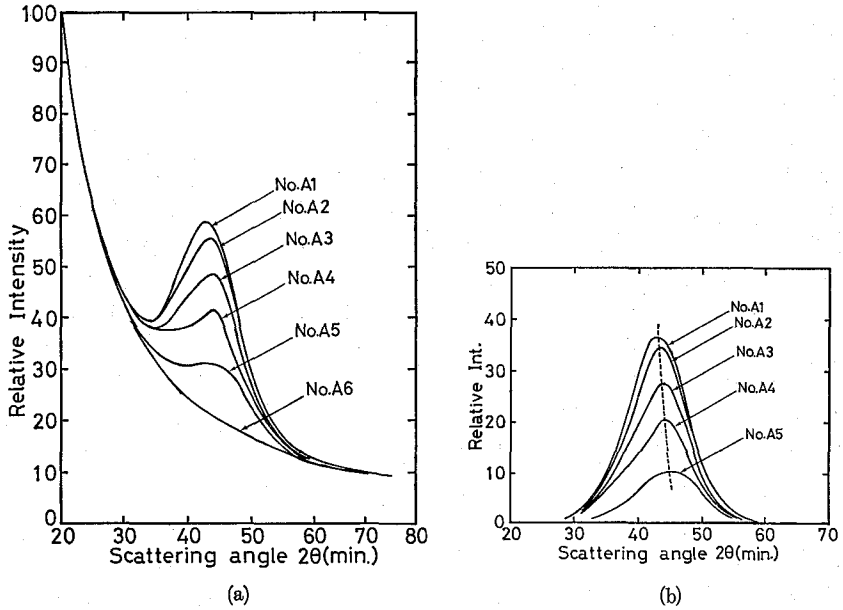

Fig. 4. (a) Normalized intensity curves of the small angle X-ray diffraction. The scale of relative intensity is arbitrary. (b) The diffraction profile obtained by subtracting the back ground intensity (No. A6) from curves of (a). The dotted line shows the peak position.

Table V. Long Period, Half-value Breadth of the DSAXD and Size of Grain of Polyethylene Single Crystal Mats of Series A

Specimen	No. A1	No. A2	No. A3	No. A4	No. A5
Long period (Å)	123	123	121	121	114
Half-value breadth (min.)	12.14	12.14	12.24	12.58	11.73
Dimension of grain (Å)	392	392	389	390	406

ized in such a way that the intensity of each curve at a diffraction angle of 20 min. is set to be 100 in arbitrary scale. As the tail of all the curves falls on a single line at the diffraction angle higher than the peak angle, this standardizing procedure can be regarded as appropriate to the comparison between these measured curves. Here, the diffraction curve of amorphous mat represents the back ground scattering of the instrumental origin including the central diffuse scattering of specimens. The line profiles in Fig. 4(b) were obtained by the subtraction of the back ground curve from the normalized curves.

The intensity of DSAXD decreases with the increase of electron irradiation. Nevertheless, the observed half-value breadth remains almost constant till the DSAXD disappears (see Table V). According to the diffraction theory of crystalline material, the broadening of line profile results from the smallness of crystallite size and/or the distortion of lattice. In view of the fact that the lamellar thickness obtained by the small angle X-ray diffraction of single crystal mat agrees well with that by electron microscopy,[13] this discrete diffraction can be regarded as the Bragg-like crystalline diffraction. For that case, the lattice spacing, lattice distortion, and crystallite size are replaced by the long period, its fluctuation and the size of a "grain" in which lamellae are coherently stacked, respectively. Since the half-value breadth in Table V remains almost constant, it is considered that the size of grain and the fluctuation of long periods are independent of electron irradiation till the crystallinity becomes vanished at the high irradiation. Assuming that the broadening of profile is caused only by the size of grain, the average size of grain can be estimated at about 390 Å from the half-value breadth by the Sherrer equation. As the fluctuation of long periods contributes to the broadening of profile, the value of breadth due to the grain size is in reality smaller and correspondingly the size of grain is larger. As the long period is 123 Å, which is estimated by applying the Bragg equation to the peak position of DSAXD, the number of lamellae consisting of a grain is estimated at 3 to 4 as an average. Thus 3∼4 lamellae are coherently stacked together. The lamellae may be stacked by the spiral growth mechanism and not by the incidental deposition of one lamella on another in the process of the formation of mat. Lamellae thus coherently stacked behave as a group for the structure deterioration by electron irradiation.

The diffraction intensity of the DSAXD decreases with the increase of radiation dose as shown in Fig. 5. The sturcture of the mat is substantially a so-called "two-phase structure": layers with crystalline and amorphous phases which correspond to the crystalline core of lamella and the interlamallar layer respecitvely are alter-

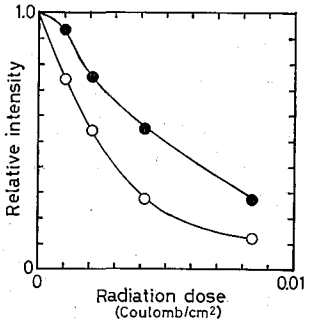

Fig. 5. The integrated intensity of discrete small angle X-ray diffraction as a function of radiation dose. The intensity of un-irradiated mat is normalized to unity. Marks ● and ○ denote the observed intensity and the intensity calculated from Eq. (3), respectively.

natively stacked in the direction normal to the mat surface. The diffraction intensity of the first order of such a layered structure is expressed as follows:[14]

$$I = N^2(\rho_c - \rho_a)^2 l_a^2 \qquad (3)$$

where N, ρ_c, ρ_a, and l_a denote the number of lamellae, the crystalline and amorphous densities and the thickness of interlamellar layer, respectively. This formula can equally be regarded as an expression of the diffraction power of the first order for a crystal which is analogous to a monoatomic crystal of simple structure and consists of N diffracting units with the scattering amplitude $|F| = (\rho_c - \rho_a) l_a$. Here, a pair of crystalline core of lamella and interlamellar layer corresponds to this diffracting unit. If a crystalline core is converted into an amorphous state with irradiation, not always a liquid-like amorphous state, so that there is not difference between the density of the converted core and that of amorphous region, then the pair of crystalline and interlamellar layers becomes a continuous single phase and is not responsible for the DSAXD, *i.e.* a non-diffracting unit. Here, it is assumed that the decrease of the degree of crystallinity, w_c, equals to the degree of conversion of the diffracting unit to the non-diffracting unit and that such non-diffracting units are randomly distributed over the mat. The structure thus assumed for the irradiated mat is analogous to that of a monoatomic crystal where there are N sites to be occupied by atoms but the w_c fraction of them is vacant (the distribution of vacanices is random). The diffraction intensity of such a monoatomic crystal is expressed by the diffraction of perfectly ordered lattice with the averaged atomic scattering amplitude reduced by a factor w_c. From the same point of view, the diffraction intensity of irradiated mat is expressed according to Eq. (3) only by replacing the structure amplitude $|F|$ with $w_c|F|$. The result of Fig. 5 obtained by using the data of Fig. 2 and Table III on this simple assumption fails to explain the decrease of the observed DSAXD intensity with irradiation. The calculated intensity largely damps, because the degree of crystallinity w_c is directly related to the intensity in the calculation by multiplying the scattering amplitude by it. Another mechanism in which the structure amplitude slowly decrease with the decrease of the degree of crystallinity or independently of it must be put forward.

One possible mechanism is the formation of continuous structure by crosslinking between molecular chains belonging to adjacent lamellae, *i.e. interlamellar crosslinking*.[15,16] When cross-links are formed between lamellae, adjacent lamellae may be forced to come near, that is, the volume of interlamellar layer decreases. Thus the density of interlamellar region increases and the thickness l_a decreases, that is, the structure amplitude decreases.

The long period decreases with irradiation (see Table V). This decrease does not always depends on the decrease of mat thickness, so that the decrease of mat thickness is due to the decrease of macroscopic void. As the long period is the sum of the lamellar thickness and the interlamellar distance, the decrease of long period is considered as caused by the decrease of the following two; (1) lamellar thickness itself and (2) interlamellar distance. Grubb *et al.* have discussed the change of lamellar thickness of polyethylene single crystal which is at the final stage of damage by electron irradiation, but here information of lamellar thickness just before the crystallinity is lost is needed. The decrease of (1) may be due mainly to intralamellar cross-linking which results in the molecular inclination in lamella. This mechanism is probable judging from the observation that the width of mat expands at high irradiation and that the molecular orientation in lamella is random as seen from a halo ring of Fig.3(a)-(4). As discussed above, the decrease of (2) is considered to be due mainly to interlamellar cross-linking. Let us consider the change in long period by both causes about the mat moderately irradiated (specimen No. A5). The long period decreases by 9 A from that of un-irradiated mat. If the molecular inclination alone causes this decrease, then the angle of tilt of stem segments at lamellar surface (fold surface) is to decrease by about 27°. Such a large molecular inclination in a lamella makes the WAXD close to the Debye-Sherrer pattern. As azimuthal spreading of diffraction arcs in Fig. 3(a)-(3) remains same as that of un-irradiated mat, Fig. 3(a)-(1), such a large change in molecular orientation does not occur and therefore it is impossible to ascribe the decrease of long period only to the molecular orientation. On the other hand, when the decrease of long period is attributed to the decrease of interlamellar distance, the distance must decrease by about 9 A. As the Moiré pattern and dislocation networks are often observed in layered polyethylene single crystals,[17] the existence of such a large clearance between stacked lamellae is considered to be less probable and therefore it is also difficult to ascribe the decrease of long period only to that of interlamellar distance. Both mechanisms must be responsible for the decrease of long period. Thus the decrease of long period is caused not only by the molecular inclination but also by shortening of interlamellar distance.

Interlamellar cross-linking produced by irradiation makes adjacent lamellae amalgamed. Since the DSAXD does not occur from these amalgamed continuous regions, the decrease of DSAXD intensity with irradiation can be explained, though qualitatively, in terms of interlamellar cross-linking. Although the intralamellar cross-linking is predominant in irradiated polymer crystals as pointed out before,[4,5] the present experiments suggests that the considerable amount of interlamellar crosslinking as well as intralamellar cross-linking exist.

Annealing

Figures 6 and 7 show three series of wide and small angle X-ray diffraction photographs which were taken of specimens damaged to various extents and annealed at various temperatures. From the comparison with these two figures, it is seen that these specimens differ from one another in annealing behavior. The difference in the behavior suggests that the structure of irradiated single crystal distinctly depends on how the specimen is damaged by electron irradiation. The DSAXD peak of un-irradiated mat(specimen of No. B1) shifts inward by annealing at high temperatures as well-known, that is, the long period of the specimen increases by annealing. As for mats damaged to lesser extent (specimen of No. B2), the WAXD and DSAXD which are slightly arced before annealing transfer into the Debye-Sherrer ring after annealing at 120°C. This change in diffraction patterns is basically distinct from that of un-irradiated specimen. The melting point

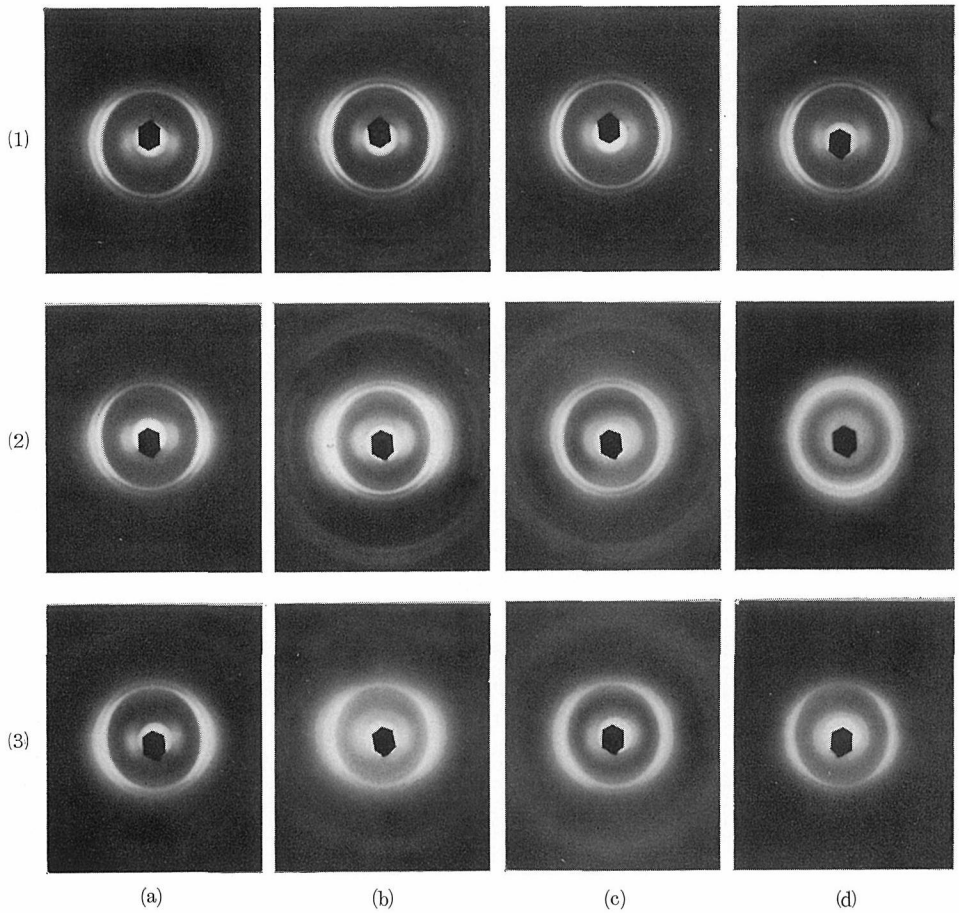

Fig. 6. Wide angle X-ray diffraction photographs of various polyethylene single crystal mats taken at various temperatures. Mats are (1) No. B1, (2) No. B2 and (3) No. B4. Temperatures are (a) room temperature, (b) 100°C, (c) 110°C and (d) 120°C. The mat is set in such a way that the normal of mat is vertical in these photographs and that the incident direction of X-ray is parallel to the mat surface.

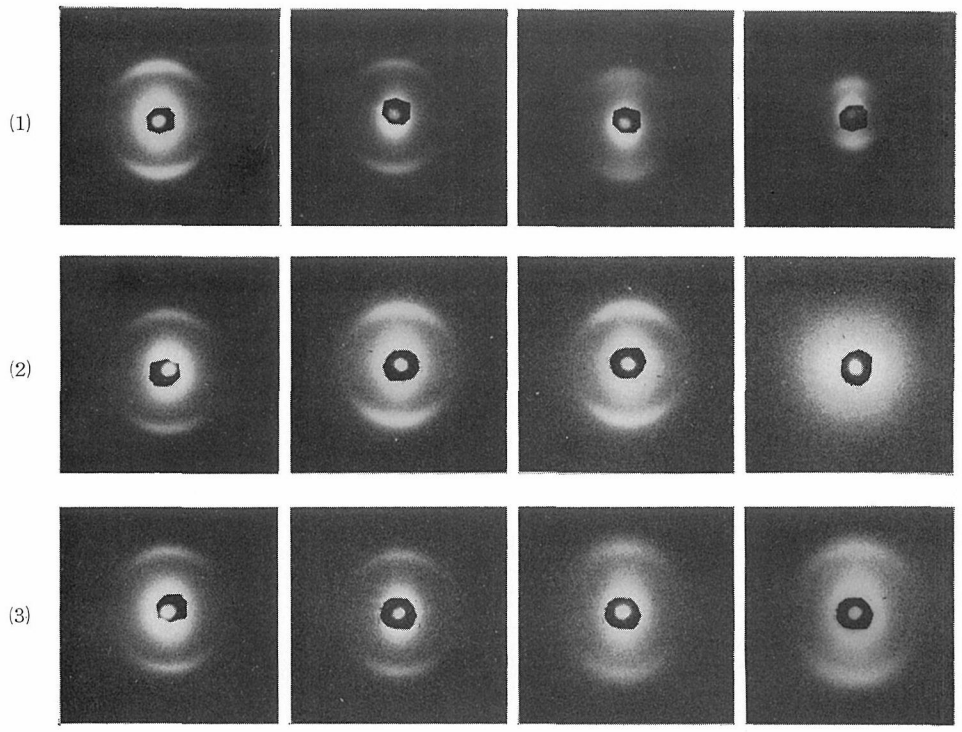

Fig. 7. Small angle X-ray diffraction photographs corresponding to Fig. 6. Setting of mats for taking these photographs is same as that in Fig. 6.

is depressed by the introduction of cross-links in crystal lattice and the melting point of this sample was found to be 116°C from the measurement by DSC. Thus the change in diffraction patterns by annealing can be interpreted in terms of melting of crystal and re-crystallization. Single crystals of specimen of No. B2 melt by annealing at 120°C, and crystallites with random orientation are formed by cooling from the melt which, though the mobility of chain is restricted by cross-links produced by electron irradiation, is isotropic. The annealing behavior of the specimen of No. B4 is quite different from above two cases. As the melting point is 109°C according to the DSC measurement, single crystals subjected to radiation damage should melt by heating above 110°C and crystallites should be formed from the melt on cooling to room temperature. Nevertheless, both WAXD and DSAXD of this annealed specimen (see Figs. 6(d) and 7(d) of series 3) are arced in the same way as those of original one. This shows that the re-crystallization of polyethylene occurs from the oriented melt and not from the isotropic melt. When cross-links are densely formed between stem segments in a lamella and between lamellae, a framework may be constructed within a lamella. The mobility of chains in the molten state of such cross-linked system is so restricted that chain segments can hardly drift away from the position registered in crystalline state. In other words, the "memory" of original crystalline state is reserved in the molten state.

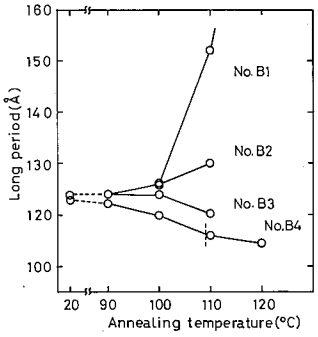

Fig. 8. Long period of various polyethylene single crystal mats as a function of annealing temperature. A short vertical dotted line shows the melting temperature of specimen of No. B4.

Figure 8 shows the change of long period of various mats by annealing. This figure also shows that single crystal mats behave in a different way depending on how they are subjected to radiation damage. The long period of un-irradiated mats increases with rising annealing temperature as previously observed.[18] The specimen slightly irradiated and maybe slightly cross-linked (specimen of No. B2) shows the slight increase of long period by annealing at a temperature below the melting temperature. The rate of the increase of long period by annealing lower than that of un-irradiated mat is clearly caused by the restriction of chain mobility due to cross-linking. The further irradiated specimen in which molecular chains are more cross-linked shows the slight decrease of long period by annealing. This decrease of long period by annealing may be caused partly by the change of the angle of tilt of molecular chain at the fold surface through the rearrangement of folds[19] and partly by the smooth contact of fold surface between adjacent lamellae, that is, the irregular fold surface produced by interlamellar cross-linking may be smoothed by equalizing the uneven fold length of stem segments. In the case of annealing of moderately irradiated mats (for example specimen of No. B4) at high temperatures, smoothing of irregular fold surface through the melting and re-crystallization process possibly accounts for the decrease of long period, since no change in molecular orientation by annealing occurs as seen in Figs. 6 and 7.

Figure 9 shows the change of lattice spacings d_{200} and d_{020} with irradiation and their annealing behavior. Correspondingly to Fig. 9, Fig. 10 shows the change of the half-value breadth of 200 reflection with irradiation and subsequent annealing. The expansion of lattice spacings with irradiation clearly accompanies the increase of half-value breadth. As previously reported,[4,5] this change is due to the introduction of lattice defects by intralamellar cross-linking. The lattice spacing d_{200} increases by annealing at low temperatures and, as the annealing temperature is rised, its magnitude reaches a maximum in a certain temperature range and decreases to a value smaller than that before annealing. On the other hand, the lattice spacing d_{020} monotonically decreases with annealing temperature. This annealing feature was first observed on un-irradiated, as-grown single crystals by Davis, Eby, and Martin[20] but this is also commonly seen in irradiated specimens. It has been point-

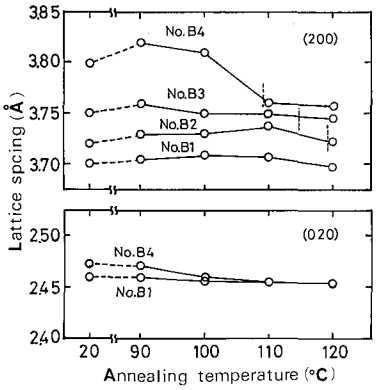

Fig. 9. Lattice spacings, d_{200} and d_{020}, of various polyethylene single crystal mats as a function of annealing temperatures. Short vertical dotted lines show the melting temperature of specimens, No. B2, No.B3 and No. B4, respectively.

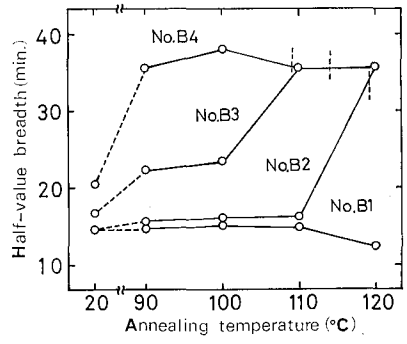

Fig. 10. Half-value breadth of various polyethylene single crystals as a function of annealing temperature. Short vertical dotted lines show the melting temperature of specimens, No. B2, No.B3 and No. B4.

ed out that this change in lattice spacing takes place by the introduction and release of defects or lattice distortion, because the tendency to increase or decrease is the same as in the half-value breadth.[21] As the edge dislocation is observed in Moiré pattern of electron micrograph of polyethylene single crystal,[22] lattice distortion is directly produced by the defects in crystalline core and also caused by the effect of the rough fold surface on the crystalline core. The rough fold surface may be formed as a result of quenching of an unstable state temporarily produced in the process to the more stable state through partial melting, since the rate of lamellar thickening is low. The annealing behavior of irradiated specimen is distinct from that of un-irradiated one: the half-value breadth keeps increasing while the lattice spacing decreases by annealing at high temperatures. Since irradiated mats have different X-ray diffraction patterns, they are apparently divided into two types from the viewpoint of diffraction behavior; (1) slightly irradiated mats and (2) moderately irradiated mats. As mentioned above, however, their annealing behavior is essentially same: annealing above the melting point is equivalent to the crystallization from the melt, while annealing below it involves the process occurring on annealing of un-irradiated specimen such as partial melting. The crystallization process of slightly cross-linked polyethylene from the melts accounts for the annealing process above the melting point of irradiated mats. The change in the half-value breadth by annealing at low temperature is the larger for highly irradiated mats. The dependence of half-value breadth on the radiation dose and annealing temperature shows that the crystal lattice of highly irradiated mat is more expanded and distorted in the process to the more stable state, because the defects may grow up and be densely distributed with long irradiation. For the fact that the half-value breadth keeps increasing despite of the decrease of the lattice spacing d_{200} by annealing at high temperatures, two causes are considered; (1) crystallites in the stable state with smaller lattice spacing becomes smaller and (2) the strain or distortion of crystal lattice is

large. As seen in Fig. 8, the long period of irradiated mats increases slightly or decreases by annealing. This shows that molecular chains hardly migrate to a distant position but only shift their positions or change their orientation around lattice points so that lamellae do not thicken (or crystallites do not grow in the direction normal to the chain axis). The interlamellar cross-linking occurs more frequently for highly irradiated mats so that lamellar surface may be more rough. Since the chain mobility is so largely restricted by inter- and intralamellar cross-linking, the lamellar surface is not fully smoothed by annealing and defects produced in crystal lattice can not be released. Moreover, since lamellar thickening does not occur, the thickness of lamella is small and therefore the surface roughness has still much effect on the crystal lattice. The structural feature of cross-linked and annealed polyethylene is very similar to that of branched low-density polyethylene. For the thermal behaviors, several works[4,23,24] are referred. The structural changes of crystal lattice due to irradiation and subsequent annealing are thus qualitatively explained in terms of crystal structure with intra- and interlamellar cross-linking.

REFERENCES

(1) A. Charlseby, "Atomic Radiation and Polymer", Pergamon, London, 1960.
(2) J.T. Judge and R.S. Stein, *J. Appl. Phys.*, **32**, 2375 (1961).
(3) H.E. Bair, R. Salovey, and T.W. Huseby, *Polymer*, **8**, 9 (1967).
(4) T. Nagasawa and K. Kobayashi, *J. Appl. Phys.*, **41**, 4276 (1970).
(5) J. Loboda-Cackvic, H. Cackovic, and R. Hosemann, *Colloid & Polymer Sci.*, **252**, 738 (1974).
(6) K. Kobayashi and K. Sakaoku, *Lab. Invest.*, **14**, 1097 (1965).
(7) H. von Orth and E.W. Fisher, *Makromol. Chem.*, **88**, 188 (1965).
(8) J.A. Venables and D.C. Bassett, *Nature*, **214**, 1107 (1967).
(9) D.T. Grubb and G.W. Groves, *Phil. Mag.*, **24**, 815 (1971).
(10) E.L. Thomas and D.G. Ast, *Polymer*, **15**, 37 (1974).
(11) D.T. Grubb, A. Keller, and G.W. Groves, *J. Mater. Sci.*, **7**, 131 (1972).
(12) Y. Nukushina, "Kobunshi Jikkenkagaku Koza", Vol. 2, ed. by S. Oka, Kyoritsushuppan, 1965.
(13) K. Kobayashi, unpublished.
(14) J.M. Shultz, W.M. Robinson, and G.M. Pound, *J. Polymer Sci: Part A-2*, **5**, 511 (1967).
(15) R. Solvey and D.C. Bassett, *J. Appl. Phys.*, **35**, 3216 (1964).
(16) T. Kawai and A. Keller, *Phil. Mag.*, **12**, 699 (1965).
(17) V.F. Holland and P.H. Lindenmeyer, *J. Appl. Phys.*, **36**, 3049 (1965).
(18) W.O. Statton and P.H. Geil, *J. Appl. Polymer Sci.*, **3**, 357 (1960).
(19) F.J. Balta Calleja, D.C. Bassett, and A. Keller, *Polymer*, **4**, 269 (1963).
(20) G.T. Davis, R.K. Eby, and G.M. Martin, *J. Appl. Phys.*, **39**, 4973 (1968).
(21) A. Kawaguchi, *Bull. Inst. Chem. Res., Kyoto Univ.*, **56**, 68 (1978).
(22) V.F. Folland, *J. Appl. Phys.*, **35**, 3235 (1964).
(23) T. Kawai and A. Keller, *Phil. Mag.*, **12**, 287 (1965).
(24) A.M. Rijke and L. Manderkern, *J. Polymer Sci.*, **B7**, 651 (1969).